Photo-Oxidation of Methanol in Complexes with Pyrido[2,3-b]pyrazine: a Nonadiabatic Molecular Dynamics Study

Electronic Supplementary Information

Joanna Jankowska*[a] and Andrzej L. Sobolewski[b]

Table of contents:

1. Natural Transition Orbitals (NTOs) calculated at the S_0-optimized PPMet stable structures

Figure S1: NTOs for PPMet-1 (ADC(2)/cc-pVDZ level of theory @ MP2/cc-pVDZ geometry).

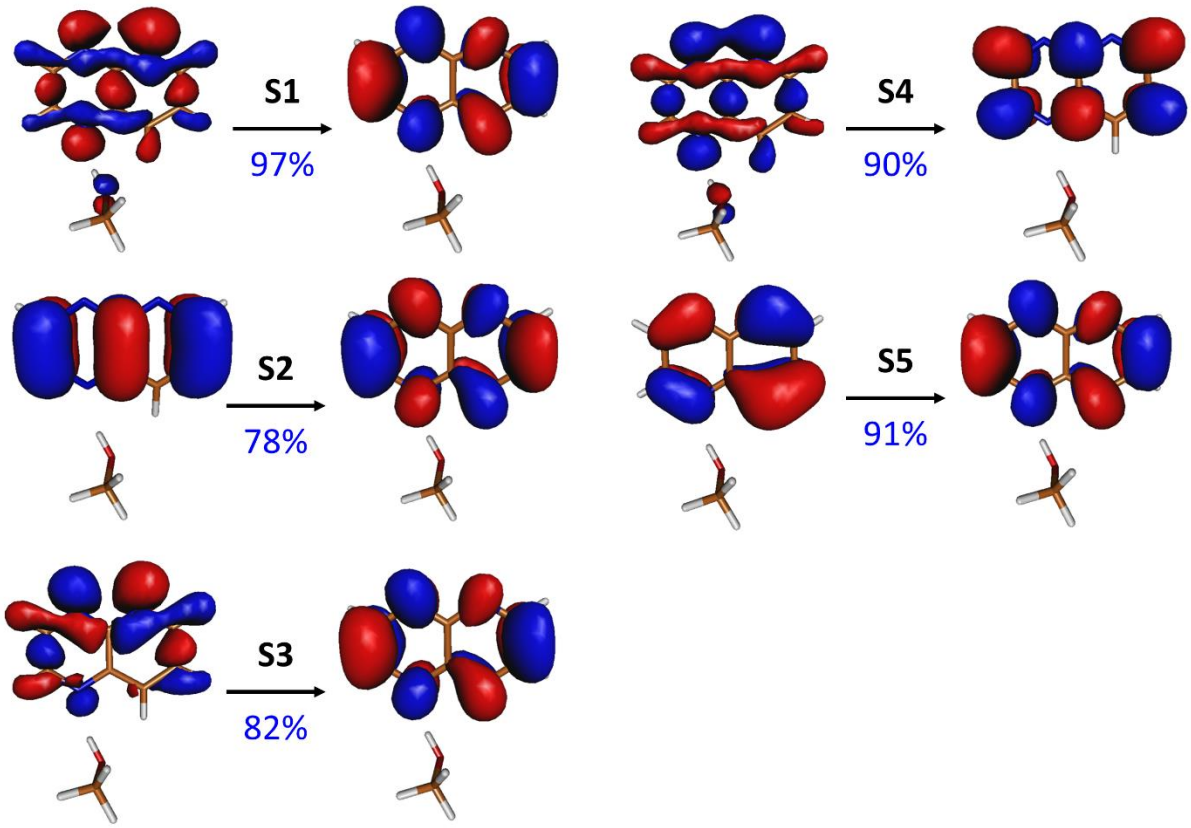

Figure S2: NTOs for PPMet-6 (ADC(2)/cc-pVDZ level of theory @ MP2/cc-pVDZ geometry).

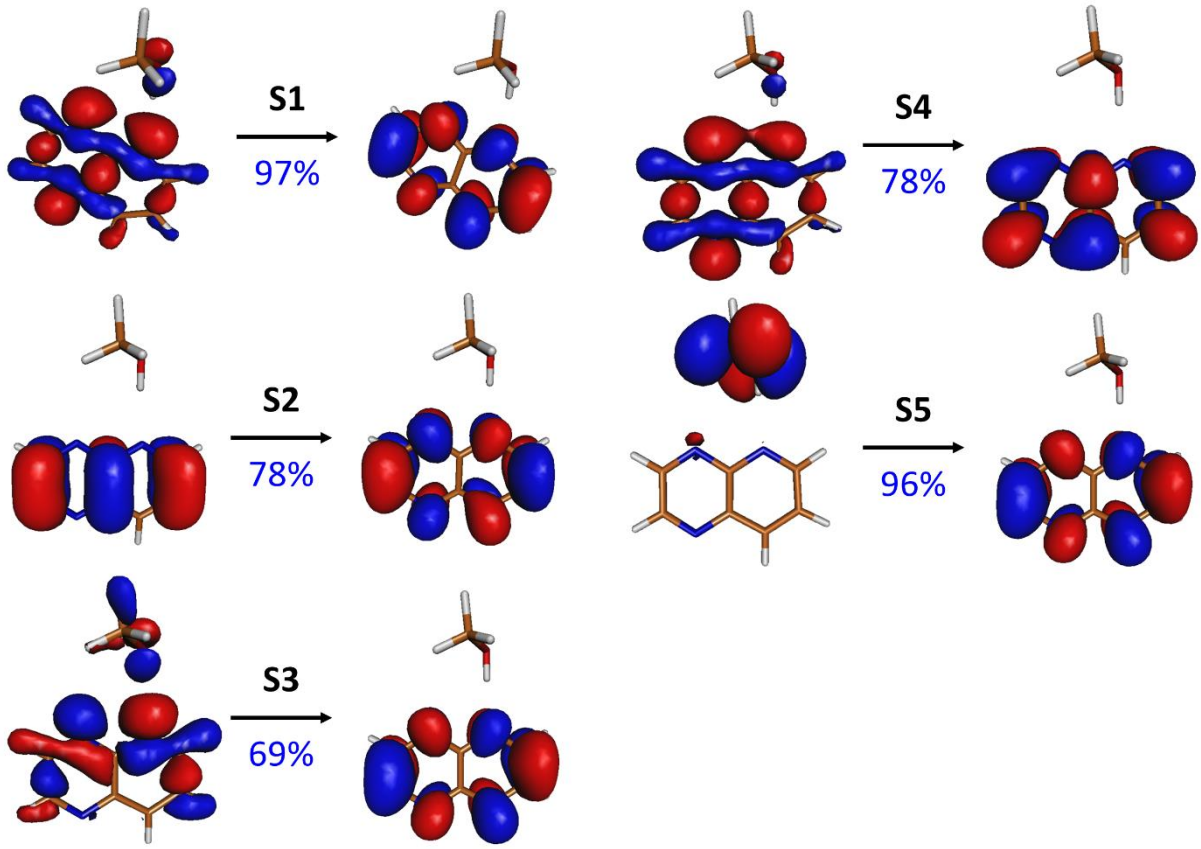

Figure S3: NTOs for PPMet-4 (ADC(2)/cc-pVDZ level of theory @ MP2/cc-pVDZ geometry).

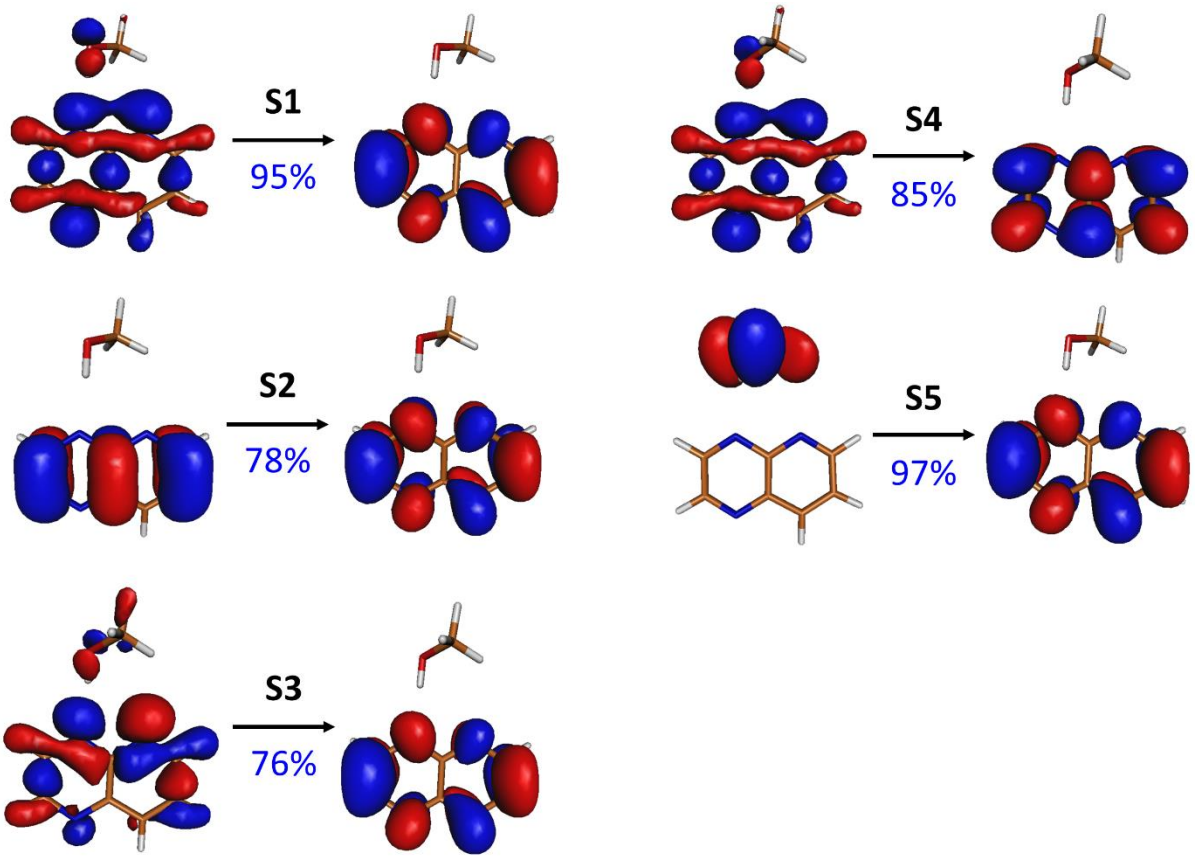

2. Natural Transition Orbitals (NTOs) calculated along direct EDPT paths for studied PPMet complexes

Figure S4: NTOs for $S_0 \rightarrow S_1$ transitions in PPMet-1, PPMet-6, and PPMet-4, calculated at selected points along the respective direct EDPT paths (ADC(2)/cc-pVDZ level of theory).

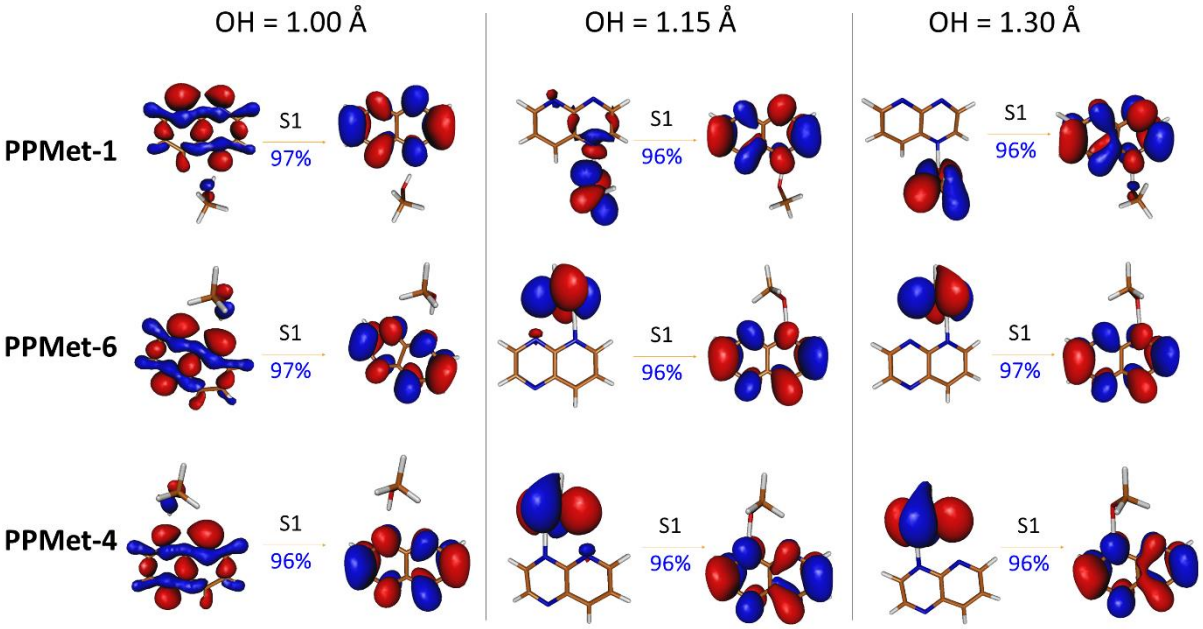

3. Charge-transfer (CT) coefficients calculated along direct EDPT paths for studied PPMet complexes

Table S1: CT coefficients for PPMet-1, PPMet-6, and PPMet-4, calculated with the TheoDORE 3.0 code at selected points along the respective direct EDPT paths (ADC(2)/cc-pVDZ level of theory). For explicit definition, please refer to Ref. 27.

CT	OH = 1.00 Å	OH = 1.15 Å	OH = 1.30 Å
PPMet-1	0.034	0.855	0.966
PPMet-6	0.067	0.982	0.990
PPMet-4	0.047	0.977	0.987

4. Single-point energy scan at the QD-NEVPT2 level performed along the direct EDPT reaction path for the PPMet-4 complex

Figure S5: Single-point QD-NEVPT2/cc-pVDZ energy scan performed along the EDPT reaction path for the PPMet-4 system. Black circles mark results obtained with the active space consisting of 8 electrons distributed in 6 orbitals (AS(8,6)), while red squares make data obtained with a larger active space, AS(16,12). Empty/full symbols indicate the S_0/S_1 energies, respectively.

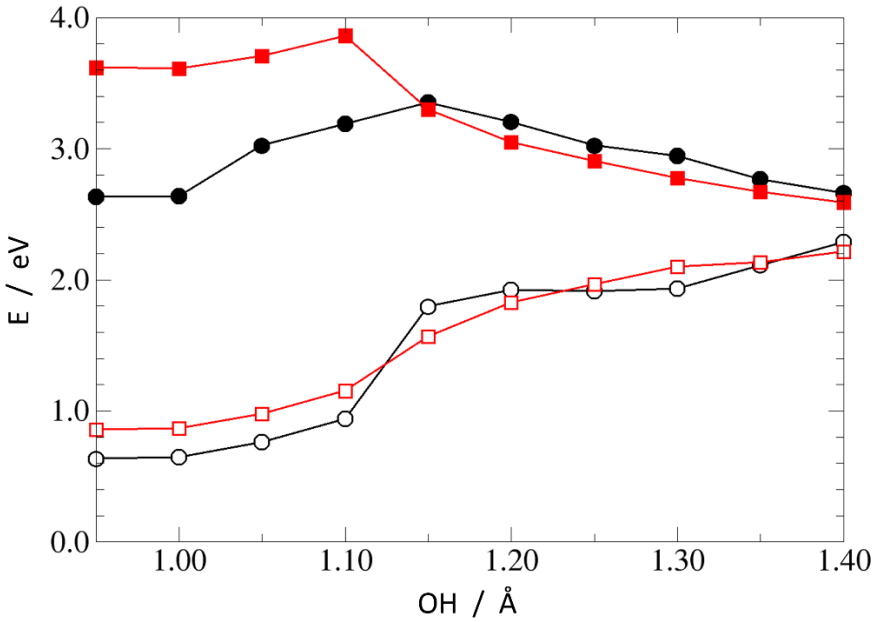

Figure S6: Active-space orbitals employed in the AS(16,12) and AS(8,6) (marked in yellow) single-point QD-NEVPT2/cc-pVDZ energy scan calculation performed along the EDPT reaction path for the PPMet-4 system, plotted for OH = 1.40 Å.

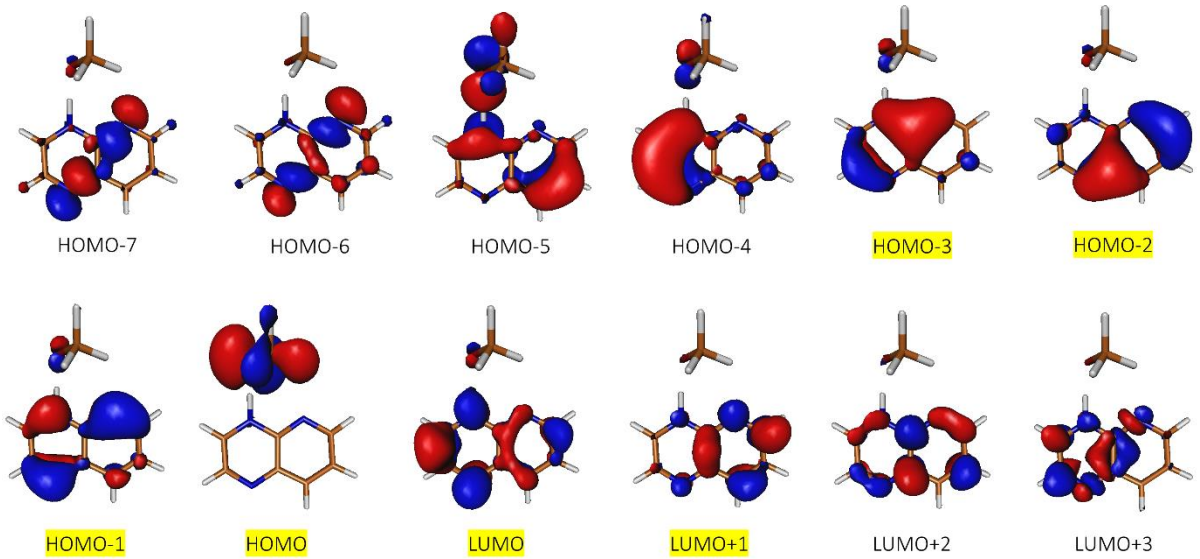

5. Relaxed EDPT reaction profiles optimize at the SCS-ADC(2) level of theory

Figure S7: EDPT reaction profiles optimized in the S_1 state at the SCS-ADC(2)/cc-pVDZ level. Black circles / red squares / blue diamonds mark results obtained for the PPMet-1 / PPMet-6 / PPMet-4 system, respectively, while the empty/full symbols indicate the S_0/S_1 energies.

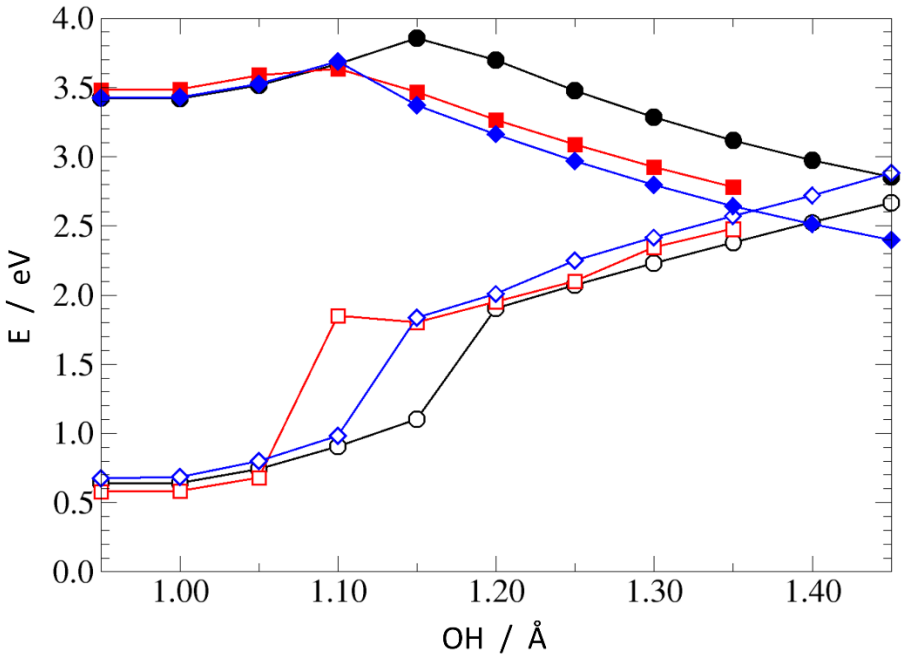

6. Optimization of MECI points for all complexes

Figure S8: Optimized MECI structures determined with the penalty-functional approach combined with the ADC(2)/cc-pVDZ method. The reported MECI energies are relative to corresponding S_0-state minima.

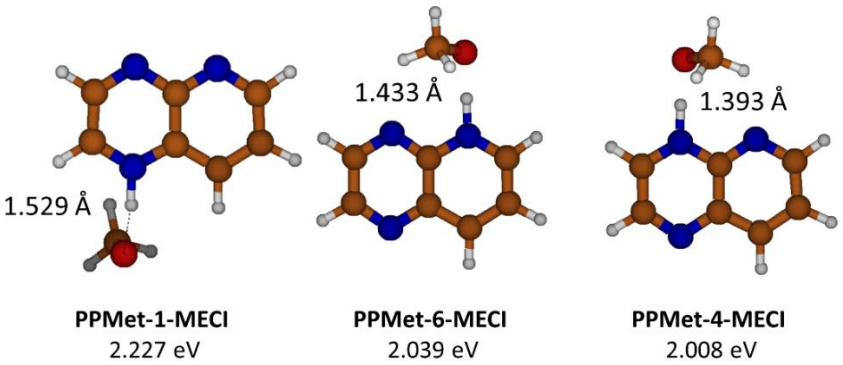

Figure S9: Molecular orbital active spaces employed in MECI optimizations performed at the XMS-CASPT2/cc-pVDZ level of theory.

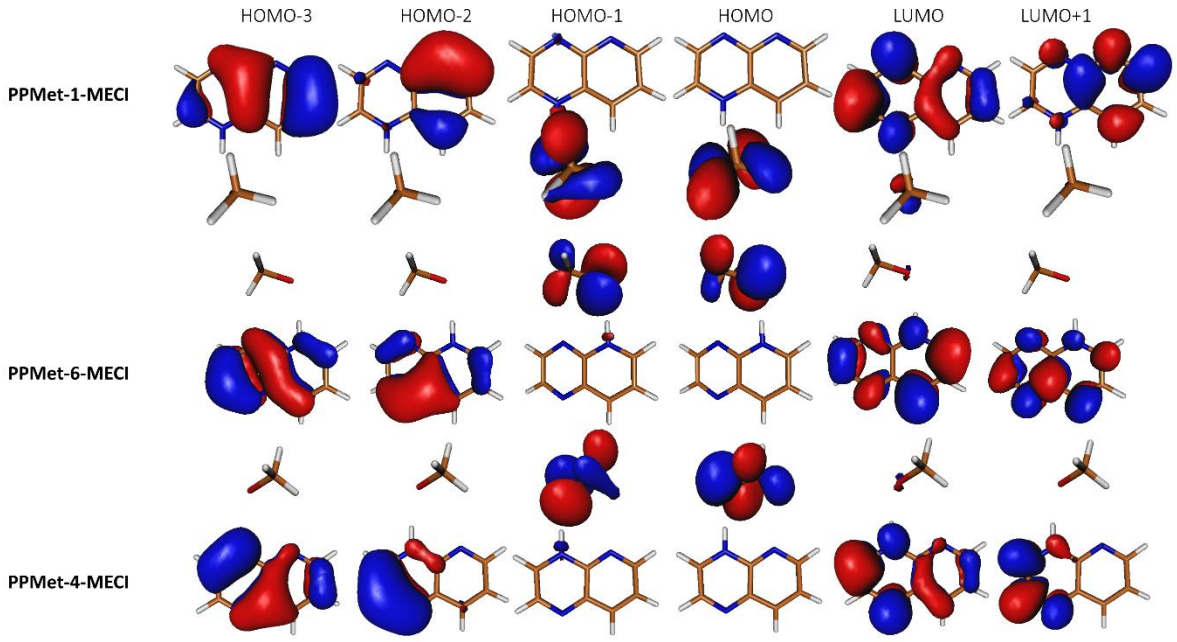

Table S2: Comparison of properties of S_1/S_0 MECI points optimized at various levels of theory. E MECI – energy of the optimized MECI with respect to the energy of the corresponding isomer S0-minimum structure; E1-E0 – energy gap at the optimized conical intersection; OH – O-H distance at MECI; NH – N-H distance at MECI, CONX – dihedral angle between the methoxy radical axis and the PP ring plane, Ex(S1) – $S_0 \longrightarrow S_1$ excitation energy.

ADC(2)/cc-pVDZ						
	E MECI (eV)	**E1-E0 (eV)**	**OH (A)**	**NH (A)**	**CONX (deg)**	**Ex(S1) (eV)**
PPMet-1	2.227	0.012	1.529	1.089	86	3.53
PPMet-4	2.008	0.008	1.393	1.147	53	3.56
PPMet-6	2.039	0.008	1.433	1.129	52	3.57
XMS-CASPT2(8in6)/cc-pVDZ						
	E MECI (eV)	**E1-E0 (eV)**	**OH (A)**	**NH (A)**	**CONX (deg)**	**Ex(S1) (eV)**
PPMet-1	2.863	0.000	2.000	1.020	81	4.31
PPMet-4	2.781	0.006	1.865	1.027	41	4.31
PPMet-6	2.641	0.001	1.964	1.023	25	4.36

7. Monoexponential fits to the S_0 state population evolution

Figure S10: The S_0-state populations extracted from the PPMet-1 (black), PPMet-6 (red), and PPMet-4 (blue) NAMD simulations (cross signs), with fitted monoexponential functions $f(t) = A \cdot \left(1 - exp\left(-\frac{t-u}{\tau}\right)\right)$ marked with solid lies, where: A – final S_0 population as $t \rightarrow \infty$, τ – combined excited state lifetime, u – fixed initial time lag before the S_0 population begins to rise. The inset shows values fitted for all isomers.

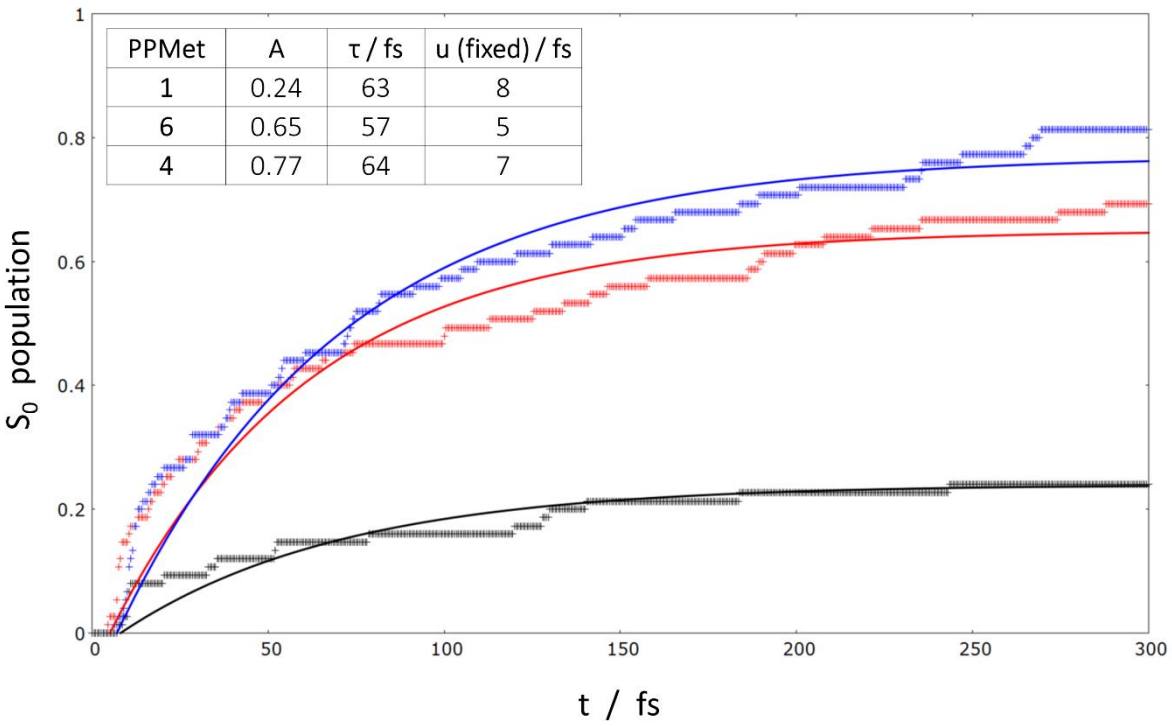

8. Initial velocity correlation analysis

Figure S11: Correlation in the PPMet-1 system between initial relative velocities of atoms involved in formation of the intermolecular hydrogen bond and: (left) the final OH distance, and (right) the duration of the simulation. Black empty circles mark data regarding the O-N relative velocity while crosses (red or blue) denote data for the N-H relative velocity.

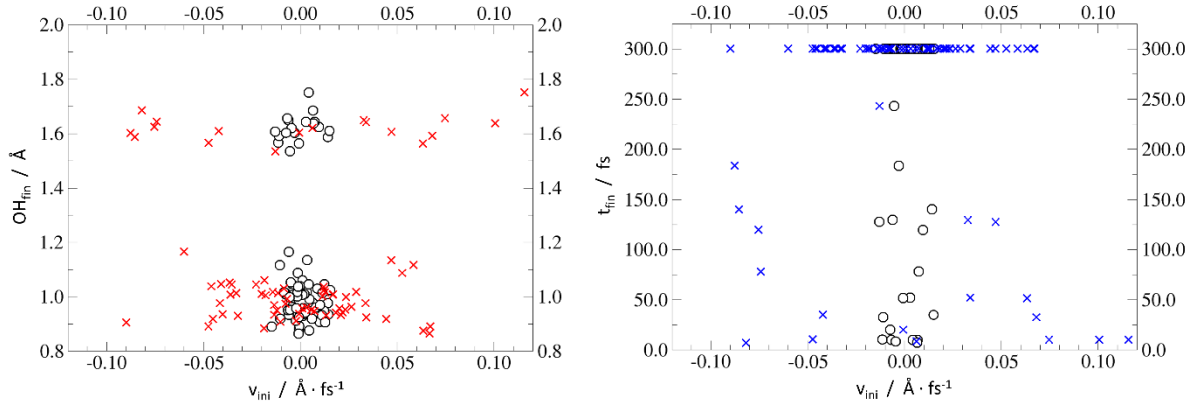

Figure S12: Correlation in the PPMet-6 system between initial relative velocities of atoms involved in formation of the intermolecular hydrogen bond and: (left) the final OH distance, and (right) the duration of the simulation. Black empty circles mark data regarding the O-N relative velocity while crosses (red or blue) denote data for the N-H relative velocity.

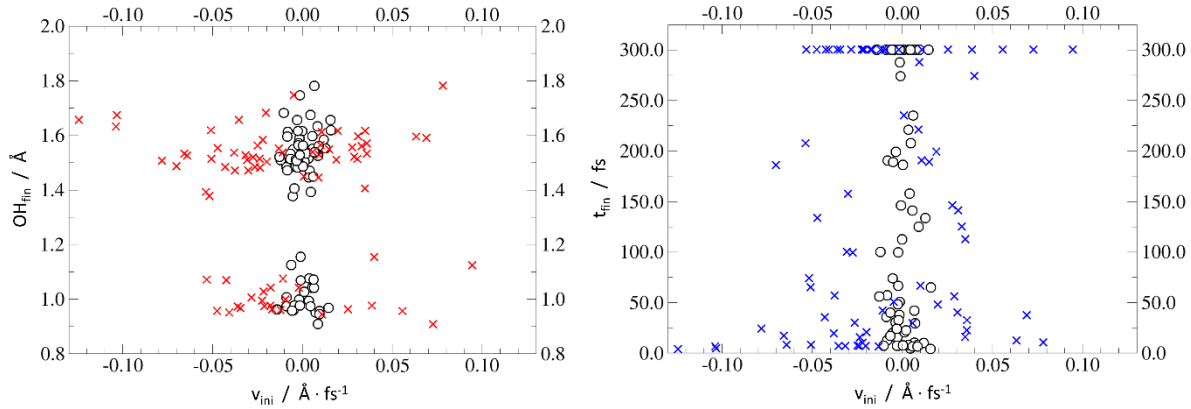

Figure S13: Correlation in the PPMet-4 system between initial relative velocities of atoms involved in formation of the intermolecular hydrogen bond and: (left) the final OH distance, and (right) the duration of the simulation. Black empty circles mark data regarding the O-N relative velocity while crosses (red or blue) denote data for the N-H relative velocity.

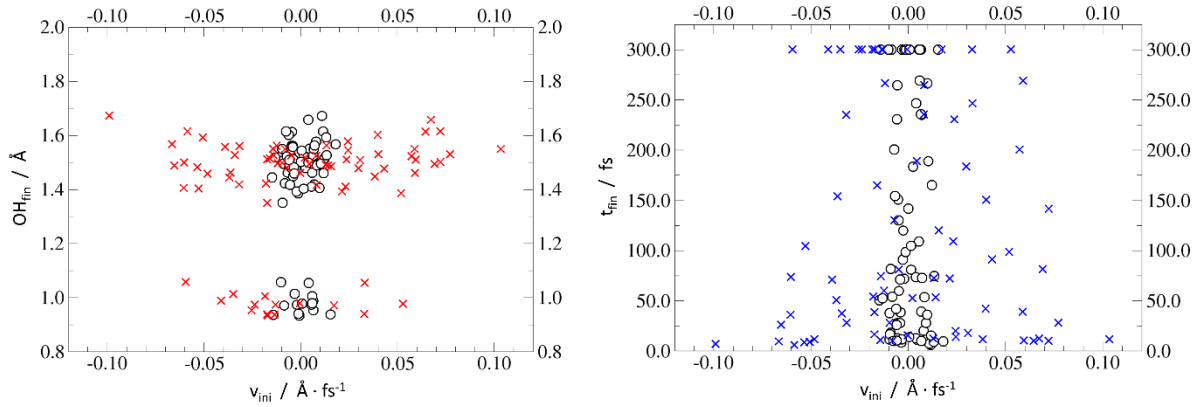

9. Visualization of short-ON hopping structures

Figure S14: Molecular geometry visualization of two PPMet structures showing short ON distance at the moment of the $S_1 \longrightarrow S_0$ hopping, with indicated relevant interatomic distances. Left/Right: structure observed in the PPMet-6 and PPMet-4 dynamics, respectively.

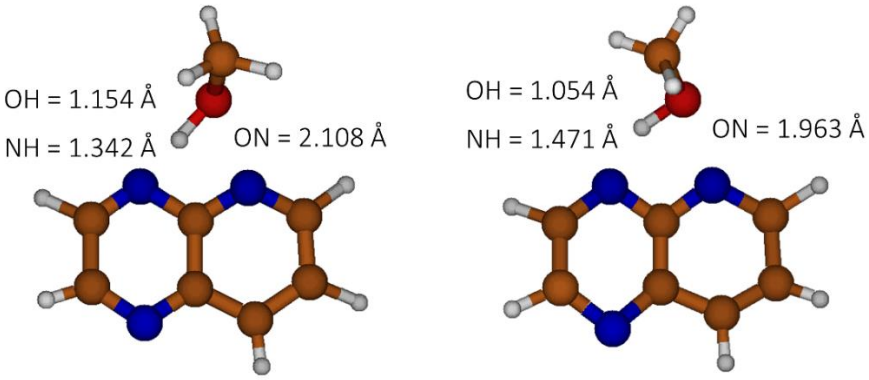

10. Correlation plot of NH distances at hopping points

Figure S15: Correlation plot of NH4 / NH6 distances at hopping points for the PPMet-6 (red diamonds) and PPMet-4 (blue crosses) dynamics.

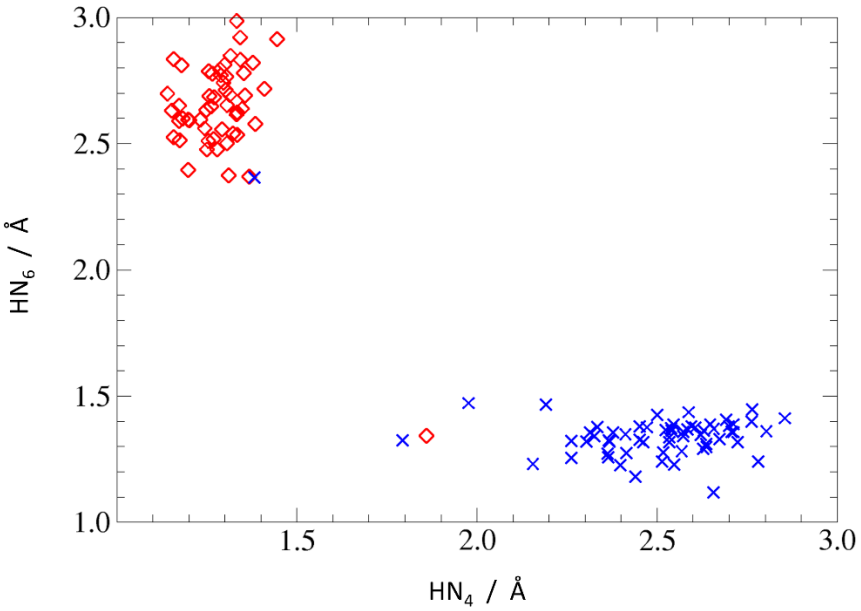

11. Cartesian coordinates of the S_0-PPMet stable structures

❖ **PPMet-1** (S0-opt: MP2/cc-pVDZ)

21

N	0.9056370	-2.6023093	-1.0910301
C	-0.1209856	-2.0054544	-0.4094863
C	0.0098304	-0.6821173	0.1355708
N	1.1701253	0.0415499	0.0060046
C	2.1523554	-0.5663810	-0.6576397
C	2.0155129	-1.8751415	-1.2009460
C	-1.0930501	-0.1100181	0.8301788
C	-2.2402225	-0.8781825	0.9476629
C	-2.2682411	-2.1832036	0.3741300
N	-1.2606671	-2.7506420	-0.2863045
O	0.5433751	2.6368814	1.1210181
C	0.2133048	3.3190800	-0.0747433
H	3.0919652	-0.0128723	-0.7740609
H	2.8554675	-2.3290791	-1.7417024
H	-0.9910664	0.8984420	1.2454899
H	-3.1773429	-2.7910670	0.4685648
H	-3.1220687	-0.4978201	1.4726001
H	0.9801318	1.8131434	0.8308591
H	-0.3369437	4.2323088	0.1998709
H	1.1076251	3.6244520	-0.6521576
H	-0.4347425	2.7184307	-0.7438793

❖ **PPMet-6** (S0-opt: MP2/cc-pVDZ)

21

N	1.1453498	0.0632501	-0.7729146
C	0.0504505	0.5322366	-0.0993751
C	0.0159889	1.8546056	0.4550089
N	1.0695580	2.7255756	0.3397326
C	2.1172012	2.2407173	-0.3236490
C	2.1554105	0.9240965	-0.8720097
C	-1.1556159	2.2680341	1.1467133
C	-2.2069253	1.3708366	1.2506800
C	-2.0764233	0.0800878	0.6627736
N	-0.9960490	-0.3405612	0.0079827
O	-0.7340837	-2.9861570	-1.2453402
C	0.4159291	-3.4848792	-0.5972530
H	2.9819240	2.9058937	-0.4394281
H	3.0497316	0.5799627	-1.4062404
H	-1.1861957	3.2764882	1.5710363
H	-2.9010161	-0.6397568	0.7343426
H	-3.1312306	1.6369917	1.7724390
H	-0.8308658	-2.0741842	-0.9181629
H	0.6086958	-4.4998437	-0.9821402
H	1.3156960	-2.8680589	-0.7875709
H	0.2924701	-3.5653355	0.5033752

❖ **PPMet-4** (S0-opt: MP2/cc-pVDZ)

21

N	1.039715	-0.123466	-0.667733
C	-0.037713	0.501087	-0.099614
C	0.000549	1.901550	0.210725
N	1.099673	2.682186	-0.040755
C	2.125887	2.037597	-0.593040
C	2.098654	0.646938	-0.904876
C	-1.151633	2.490710	0.800512
C	-2.247288	1.677814	1.042551
C	-2.177498	0.296431	0.695413
N	-1.120786	-0.295542	0.142237
O	0.673699	-3.010350	-1.296863
C	0.176838	-3.572749	-0.101304
H	3.024565	2.628179	-0.809712
H	2.972009	0.164313	-1.359969
H	-1.132010	3.558322	1.040752
H	-3.042300	-0.351437	0.885715
H	-3.161034	2.076230	1.494353
H	0.741738	-2.055264	-1.125609
H	0.041135	-4.653868	-0.268969
H	0.873431	-3.454653	0.755241
H	-0.797631	-3.144029	0.200944